Bit-Wise Partial Noise Elimination in Cooperative Decode-Amplify-Forward Relay Node

Shinsuke Ibi, Naoyuki Takada, and Seiichi Sampei
Dept. of Information and Communications Technol.,
Osaka Univesity, 2-1 Yamada-oka, Suita, 565–0871, Japan
Email: {ibi, sampei}@comm.emg.osaka-u.ac.jp

***Abstract*—This paper deals with an adaptive bit-wise switching strategy for hybrid decode-forward (DF) and decode-amplify-forward (DAF) relaying and proposes a novel bit-wise partial noise elimination technique. In relay nodes of DAF relaying, bit log likelihood ratios (LLR)s with high reliability is proactively hard-decoded to cut noise propagation. With this method, we have a difficulty to calculate LLRs in the destination node, due to multi-modality of probability density function (PDF) caused by nonlinear operations of the noise elimination. In order to resolve this issue, a classification problem is formulated in this paper.**

We will demonstrate that DAF with the bit-wise noise elimination functionality is capable of improving frame error rate (FER) performance in the destination node.

I. Introduction

Cooperative relaying has attracted a significant research attention owing to its spatial diversity benefits to remedy path-loss and shadowing as well as fading issues [1]–[3]. In principle, the spatial diversity is obtained by a collection of distributed terminals which assist one another. The simplest form of the cooperative system is triangle topology constituted by a source (S) a relay (R) and a destination (D). The concepts behind user cooperation is originated and motivated in 1970s significant theoretic advances on relay channels [4], [5]. Main outcomes of the classical studies are on three types of relaying strategy: *amplify-forward* (AF), *decode-forward* (DF), and *compress-forward* (CF).

In the AF manner, the R node forwards analog waveforms reached from the S node, while amplifying the received signals. Computational burden involved in the AF relaying is extremely small, but noise components added in the R node are always propagated to the D node even when signal-to-noise power ratio (SNR) of the S-R pair is high. In order to eliminate the propagated noise components, the DF relaying decodes into the source message. The decoded message is re-encoded before being forwarded to the D node. However, there is a danger to include decoding errors in the case where the SNR of the S-R pair is low. As the result, decoding errors are propagated to the D node. The tradeoff of noise and error propagations implies a fact that AF and DF relaying should be switched according to the SNR of S-R pair for each frame (or packet), as proposed in [6].

AF relaying may be regarded as a way of forwarding soft reliability information without utilizing channel codec. Since the channel encoder may be often utilized in the S node, a channel decoder in the R node is capable of yielding extrinsic log likelihood ratio (LLR) as the soft reliable information. Although computational burden in the R node increases, the LLRs after forward error corrections should be forwarded to attain high detection capability, instead of the analog waveform. This strategy is referred to as *Decode-amplify-forward* (DAF) [7]. With the aid of DAF strategy, an adaptive DAF-DF switching according to the SNR of S-R pair for each frame may experience an improvement of detection capability.

A primary focus of this paper is on an efficient adaptive switching strategy for hybrid DAF and DF relaying, and contributions are as following:

- We propose a bit-wise partial noise elimination methodology for DAF relaying. Bit LLRs with high reliability is proactively hard-decoded by following the philosophy of DF relaying, resulting in the noise elimination. The other LLRs are forwarded by following the philosophy of DAF relaying.
- We solve a classification problem which is faced in the D node: we have to know which received bits are free from the noise propagation issue. Probability density function (PDF) of the received signal obeys Gaussian mixture models, due to the noise elimination in the R node. The classification allows us to calculate LLRs with reasonable computational efforts.

The rest of this paper is organized as follows. In Sect. II, the problems to be solved in this paper are clarified in the context of the system models of cooperative relaying. Then, a novel bit-wise partial noise elimination scheme is proposed in Sect. III. The scheme is characterized with the aid of computer simulations in Sect. IV. Finally, the paper is concluded by a brief summary in Sect. V.

II. System Model

A. Channel model of cooperative relaying

A simple triangular topology for cooperative relaying is considered in this paper. In a broadcast (the first) phase, R and D nodes simultaneously receive symbols $y_{\mathrm{R}}^{\mathrm{B}}(k)$ and $y_{\mathrm{D}}^{\mathrm{B}}(k)$ as a consequence of symbol $x_{\mathrm{S}}^{\mathrm{B}}(k)$ radiations from S node. Note that k denotes a discrete index. After generating appropriate symbols $x_{\mathrm{R}}^{\mathrm{C}}(k)$ (with DF or DAF manner) according to the received symbols $y_{\mathrm{R}}^{\mathrm{B}}(k)$ in the R node, the D node obtains received symbols $y_{\mathrm{D}}^{\mathrm{C}}(k)$ in a following cooperative (the second) phase.

978-1-4673-0990-5/12/$31.00 ©2012 IEEE

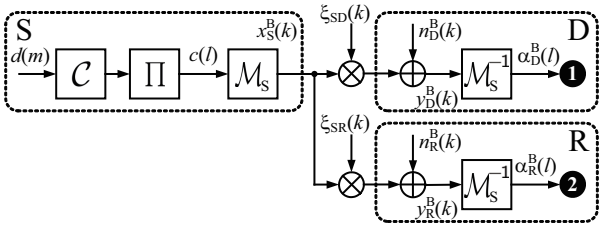

(a) Broadcast phase.

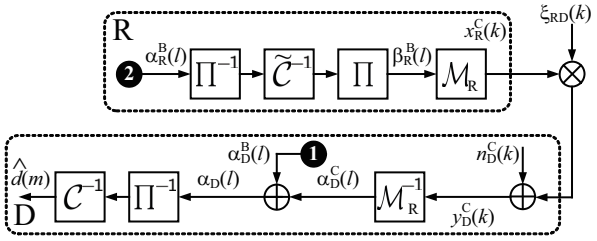

(b) Cooperative phase.

Fig. 1. Schematic of transceiver. $\mathcal{C}$ and $\mathcal{C}^{-1}$ denote channel encoder and decoder. $\tilde{\mathcal{C}}^{-1}$ indicates MAP decoder to yield extrinsic LLRs with respect to coded bits. Π and Π^{-1} are interleaver and deinterleaver, respectively. $\mathcal{M}_{\rm S}$ and $\mathcal{M}_{\rm S}^{-1}$ denote bit-to-symbol mapper and symbol-to-LLR demapper. $\mathcal{M}_{\rm R}$ and $\mathcal{M}_{\rm R}^{-1}$ denote LLR-to-symbol mapper and its inverse operation.

Utilizing OFDM systems as a means to support broadband wireless communications, parallel Rayleigh fading channels are readily created by fast Fourier transform (FFT) operations with the aid of cyclic prefix. The OFDM signaling utilizes K subcarriers and the cyclic prefix with length N, resulting in $(K+N)$ frame length. Let the joint impacts of path loss, shadowing, and flat fading over the k-th subcarrier of S-R, S-D, and R-D pairs be denoted by the coefficients $\xi_{\rm SR}(k)$, $\xi_{\rm SD}(k)$, and $\xi_{\rm RD}(k)$, respectively. In the broadcast phase, the received symbols $y_{\rm R}^{\rm B}(k)$ and $y_{\rm D}^{\rm B}(k)$ are expressed as

$$y_{\rm R}^{\rm B}(k) = \xi_{\rm SR}(k)x_{\rm S}^{\rm B}(k) + n_{\rm R}^{\rm B}(k), \quad (1)$$

$$y_{\rm D}^{\rm B}(k) = \xi_{\rm SD}(k)x_{\rm S}^{\rm B}(k) + n_{\rm D}^{\rm B}(k), \quad (2)$$

where $n_{\rm R}^{\rm B}(k)$ and $n_{\rm D}^{\rm B}(k)$ are random variables obeying identical complex-valued white Gaussian noise process of $\mathcal{CN}(0, N_0)$, and N_0 denotes the one-sided noise power spectral density. Similarly, in the cooperative phase, the received symbols $y_{\rm D}^{\rm C}(k)$ is given by

$$y_{\rm D}^{\rm C}(k) = \xi_{\rm RD}(k)x_{\rm R}^{\rm C}(k) + n_{\rm D}^{\rm C}(k), \quad (3)$$

where $n_{\rm D}^{\rm C}(k)$ is also a random variable obeying $\mathcal{CN}(0, N_0)$.

B. Broadcast phase

A schematic of transceiver in the broadcast phase is depicted in Fig. 1(a). Each frame to be conveyed to the D node contains K coded data symbols $x_{\rm S}^{\rm B}(k)$. In order to generate the frame in the S node, a binary information sequence $d(m) \in \{0,1\}$ $(m = 1, \ldots, 2KR_{\rm c})$ is convolutionaly encoded $(\mathcal{C})$ with code rate $R_{\rm c}$ and randomly interleaved (Π), resulting in a sequence of coded bit $c(l) \in \{0,1\}$ $(l = 1, \ldots, L(= 2K))$. After quadrature phase shift keying (QPSK) with Gray labeling $(\mathcal{M}_{\rm S})$, the data symbols are embedded in the frame, as coded data symbols $x_{\rm S}^{\rm B}(k)$. Note that the Gray coded labeling is comprised of phases $\mathcal{S} = \{\mathcal{S}_0, \mathcal{S}_1, \mathcal{S}_2, \mathcal{S}_3\} = \{(-1 - {\rm j})w_x, (-1 + {\rm j})w_x, (1 - {\rm j})w_x, (1 + {\rm j})w_x\}$ where ${\rm j} = \sqrt{-1}$, $w_x = \sqrt{E_{\rm s}/2}$ and $E_{\rm s}$ is the energy of each data symbol. Subsequently, K-point inverse FFT (IFFT) is carried out, and cyclic prefix is inserted.

The received symbols after cyclic prefix removal and K-point FFT are given by (1) and (2) under the assumption that the channel memory length of channel impulse response (CIR) is less than N. The symbol-to-log likelihood ratio (LLR) demapper $(\mathcal{M}_{\rm S}^{-1})$ of the R and D nodes calculates extrinsic LLRs $\alpha_j^{\rm B}(l)$ $(j \in \{{\rm R}, {\rm D}\})$, which are defined by

$$\begin{aligned}\alpha_j^{\rm B}(l) &= \ln \frac{\Pr[y_j^{\rm B}(k)|c(l)=1]}{\Pr[y_j^{\rm B}(k)|c(l)=0]} \\ &\approx \ln \frac{\sum_{\mathcal{S}_q \in \{\mathcal{S}|c(l)=1\}} p(y_j^{\rm B}(k)|\mathcal{S}_q)}{\sum_{\mathcal{S}_{q'} \in \{\mathcal{S}|c(l)=0\}} p(y_j^{\rm B}(k)|\mathcal{S}_{q'})}, \end{aligned} \quad (4)$$

where $\mathcal{S}_q \in \{\mathcal{S}|c(l)=b\}$ indicates subset of $\mathcal{S}$ belonging to $c(l)=b$. The probability density function (PDF) $p(y_j^{\rm B}(k)|\mathcal{S}_q)$ is given by

$$p(y_j^{\rm B}(k)|\mathcal{S}_q) = \frac{1}{\pi N_0} \exp\left(-\frac{|y_j^{\rm B}(k) - \xi_{{\rm S}j}(k)\mathcal{S}_q|^2}{N_0}\right). \quad (5)$$

The Gray coded QPSK labeling allows us to rewrite (4) as

$$\boldsymbol{\alpha}_j^{\rm B}(k) = \omega_\alpha \boldsymbol{\eta}_{{\rm S}j}(k), \quad (6)$$

where we have

$$\boldsymbol{\alpha}_j^{\rm B}(k) = \left[\alpha_j^{\rm B}(l=2k-1), \alpha_j^{\rm B}(l=2k)\right]^{\rm T}, \quad (7)$$

$$\omega_\alpha = \frac{4w_x}{N_0} = \frac{2\sqrt{2E_s}}{N_0}, \quad (8)$$

$$\boldsymbol{\eta}_{{\rm S}j}(k) = \left[\Re\left[\xi_{{\rm S}j}^*(k)y_j^{\rm B}(k)\right], \Im\left[\xi_{{\rm S}j}^*(k)y_j^{\rm B}(k)\right]\right]^{\rm T}. \quad (9)$$

Note that $\Re[\cdot]$ and $\Im[\cdot]$ denote real and imaginary parts of complex values, respectively. $\cdot^*$ indicates conjugate.

C. Cooperative phase

A schematic of transceiver in the cooperative phase is depicted in Fig. 1(b). In the relay transmission, the R node plays a key role of the cooperation. In the R node, error corrections are carried out by channel decoding process while observing a sequence of extrinsic LLRs $\boldsymbol{\alpha}_{\rm R}^{\rm B} = \left[\alpha_{\rm R}^{\rm B}(1), \ldots, \alpha_{\rm R}^{\rm B}(L)\right]$. As the result, we have the other extrinsic LLR $\beta_{\rm R}^{\rm B}(l)$ with respect to coded bits $c(l)$, which is defined by

$$\beta_{\rm R}^{\rm B}(l) = \ln \frac{\Pr\left[c(l)=1|\boldsymbol{\alpha}_{\rm R}^{\rm B}\right]}{\Pr\left[c(l)=0|\boldsymbol{\alpha}_{\rm R}^{\rm B}\right]} - \alpha_{\rm R}^{\rm B}(l). \quad (10)$$

The extrinsic LLR $\beta_{\rm R}^{\rm B}(l)$ is calculated by BCJR algorithm based Maximum *A-Posteriori* (MAP) decoding with the aid of interleaver and deinterleaver $(\Pi^{-1}, \tilde{\mathcal{C}}^{-1}, \Pi)$. It is well kwon that the BCJR algorithm is a powerful tool to calculate marginal probability by focusing on Trellis structure of the channel code without requiring a huge amount of computational effort. However, in order to avoid the computational burden involved in the error corrections, we may omit the

MAP decoding, resulting in $\beta_{\rm R}^{\rm B}(l) = \alpha_{\rm R}^{\rm B}(l)$, instead of (10), while allowing a sacrifice of detection capability in the D node.

The derived extrinsic LLR $\beta_{\rm R}^{\rm B}(l)$ is provided to LLR-to-symbol mapper ($\mathcal{M}_{\rm R}$) for the sake of producing forwarded data symbols $x_{\rm R}^{\rm C}(k)$, according to DF or DAF manner. Then, its inverse operation ($\mathcal{M}_{\rm R}^{-1}$) is applied in the D node to calculate extrinsic LLRs $\alpha_{\rm D}^{\rm C}(l)$. The derivations of $x_{\rm R}^{\rm C}(k)$ and $\alpha_{\rm D}^{\rm C}(l)$ are detailed in later. Subsequently, demapper outputs of broadcast and cooperative phases are combined to obtain cooperation effects, expressed as

$$\alpha_{\rm D}(l) = \alpha_{\rm D}^{\rm B}(l) + \alpha_{\rm D}^{\rm C}(l). \tag{11}$$

The combination of LLRs indicates a decoding operation of repetition codes which is composed of coded bits over broadcast and cooperation phases. After deinterleaving (Π^{-1}) the combined LLRs $\alpha_{\rm D}(l)$, MAP decoding ($\mathcal{C}^{-1}$) is carried out to detect information bit $d(m)$.

1) DF manner: Each extrinsic LLR $\beta_{\rm R}^{\rm B}(l)$ is hard-decoded to bit $\hat{c}(l)$. According to the derived hard-bit, QPSK with Gray labeling is applied to obtain the forwarded data symbols $x_{\rm R}^{\rm C}(k)$. In the D node, observing received symbols $y_{\rm R}^{\rm C}(k)$, the symbol-to-LLR demapper may yield extrinsic LLRs $\alpha_{\rm D}^{\rm C}(l)$, which are defined by

$$\alpha_{\rm D}^{\rm C}(l) \;=\; \ln \frac{\Pr[y_{\rm R}^{\rm C}(k)|c(l)=1]}{\Pr[y_{\rm R}^{\rm C}(k)|c(l)=0]}. \tag{12}$$

While ignoring hard decision errors including in $\hat{c}(l)$, we have $c(l) \approx \hat{c}(l)$. Under this rough approximation, as with the derivation of (6), (12) is rewritten as

$$\boldsymbol{\alpha}_{\rm D}^{\rm C}(k) \approx \omega_\alpha \boldsymbol{\eta}_{\rm RD}(k), \tag{13}$$

where we have

$$\boldsymbol{\alpha}_{\rm D}^{\rm C}(k) \;=\; \left[\alpha_{\rm D}^{\rm C}(l=2k-1), \alpha_{\rm D}^{\rm C}(l=2k)\right]^{\rm T}, \tag{14}$$

$$\boldsymbol{\eta}_{\rm RD}(k) \;=\; \left[\Re\left[\xi_{\rm RD}^{*}(k) y_{\rm D}^{\rm B}(k)\right], \Im\left[\xi_{\rm RD}^{*}(k) y_{\rm D}^{\rm B}(k)\right]\right]^{\rm T}. \tag{15}$$

Unfortunately, the above mentioned approximation is not always satisfied. Especially, low received $E_{\rm s}/N_0$ over S-R link sensitively deteriorates an accuracy of the approximation.

2) DAF manner: Extending the binary phase shift keying (BPSK) based DAF in [7] to a Gray coded QPSK senario, the forwarded data symbol $x_{\rm R}^{\rm C}(k)$ may be obtained by simple linear algebra:

$$x_{\rm R}^{\rm C}(k) = \frac{w_x}{\sqrt{\overline{P_\beta}}}\left(\beta_{\rm R}^{\rm B}(l=2k-1) + {\rm j}\beta_{\rm R}^{\rm B}(l=2k)\right), \tag{16}$$

where we have $\overline{P_\beta} = \frac{\sum_{l=1}^{L} |\beta_{\rm R}^{\rm B}(l)|^2}{L}$.

We assume here that the extrinsic LLR $\beta_{\rm R}^{\rm B}(l)$ may be regarded as the received constellation points of BPSK signaling over Gaussian channels [8], as defined by

$$\beta_{\rm R}^{\rm B}(l) \approx \mu\tilde{c}(l) + \nu(l), \tag{17}$$

where $\tilde{c}(l) = 2c(l) - 1$ and $\nu(l)$ represents a random variable obeying the zero-mean real-valued white Gaussian noise process of $\mathcal{N}(0, \sigma_\beta^2)$. Substituting (17) into (16), we have

$$x_{\rm R}^{\rm C}(k) \approx \tilde{\mu} x_{\rm S}^{\rm B} + w_x \tilde{n}_\beta(k), \tag{18}$$

where $\tilde{\mu} = \frac{\mu}{\sqrt{\overline{P_\beta}}}$ and $\tilde{n}_\beta(k) = \frac{\nu(2k-1)+{\rm j}\nu(2k)}{\sqrt{\overline{P_\beta}}}$ obeying $\mathcal{CN}\left(0, 2\tilde{\sigma}_\beta^2\left(=2\frac{\sigma_\beta^2}{\overline{P_\beta}}\right)\right)$. Consequently, (3) is rewritten as

$$y_{\rm D}^{\rm C}(k) = \xi_{\rm RD}(k)\tilde{\mu} x_{\rm S}^{\rm B}(k) + \xi_{\rm RD}(k) w_x \tilde{n}_\beta(k) + n_{\rm D}^{\rm C}(k), \tag{19}$$

Since the second and third terms on the right-hand in (19) are independent, variance of the unified noise term is $N_0 + 2\tilde{\sigma}_\beta^2 |\xi_{\rm RD}(k)|^2 w_x^2$. As with the derivation of (6), (12) is given by

$$\boldsymbol{\alpha}_{\rm D}^{\rm C}(k) = \omega_{\rm DAF}(k)\boldsymbol{\eta}_{\rm RD}(k), \tag{20}$$

where

$$\omega_{\rm DAF}(k) = \frac{4 w_x \tilde{\mu}}{N_0 + 2\tilde{\sigma}_\beta^2 |\xi_{\rm RD}(k)|^2 w_x^2}. \tag{21}$$

Note that the information of $\tilde{\mu}$ and $\tilde{\sigma}_\beta^2$ should be notified to the D node. The notification is assumed to be perfect for the ease of analysis in this paper. As a demerit of DAF method, noise terms are always delivered to the D node, even if some highly reliable LLRs are obtained after error corrections in the R node. The disadvantageous point simply implies that noise terms of reliable LLR should be proactively eliminated by hard decision in the DF manner. In other words, the noise term included in lowly reliable LLRs should be conveyed by DAF.

III. Bit-Wise Partial Noise Elimination for DAF

A simple and straight-forward method to eliminate noise terms in reliable LLRs is to exploit an LLR threshold value $L_{\rm th}$, expressed as

$$\hat{b}(l) = \begin{cases} 1 & (L_{\rm th} \le \beta_{\rm R}^{\rm B}(l)) \\ \beta_{\rm R}^{\rm B}(l)/\mu & (-L_{\rm th} < \beta_{\rm R}^{\rm B}(l) < L_{\rm th}) \\ -1 & (\beta_{\rm R}^{\rm B}(l) \le -L_{\rm th}). \end{cases} \tag{22}$$

In order to know information of μ in the R node, we assume here a consistency condition of extrinsic LLR which is identical to a relation given by $\mu = 2\sigma_\beta^2$ [9]. Since the variance σ_β^2 is calculated by

$$\sigma_\beta^2 (= 2\mu) = \overline{P_\beta} - \mu^2. \tag{23}$$

Thus, μ is given by $\mu = \sqrt{1 + \overline{P_\beta}} - 1$.

Based on the bit-wise partial noise eliminated signals $\hat{b}(l)$, tentative forwarded data symbols $\hat{x}_{\rm R}^{\rm C}(k)$ is produced by

$$\hat{x}_{\rm R}^{\rm C}(k) \;=\; \left(\hat{b}(l=2k-1) + {\rm j}\hat{b}(l=2k)\right). \tag{24}$$

Subsequently, averaged enregy is amplified to $E_{\rm s}$, expressed as

$$x_{\rm R}^{\rm C}(k) \;=\; \hat{x}_{\rm R}^{\rm C}(k) w_x \quad \text{if} \quad |\hat{x}_{\rm R}^{\rm C}(k)| = 2. \tag{25}$$

Otherwise, i.e. for symbols including soft-valued $\hat{b}(l)$,

$$x_{\rm R}^{\rm C}(k) = \hat{x}_{\rm R}^{\rm C}(k) w_{\rm NE}, \tag{26}$$

where $w_{\rm NE} = \sqrt{E_{\rm s}/\overline{P_{\rm NE}}}$ and $\overline{P_{\rm NE}}$ is energy averaged over all tentative symbols $\hat{x}_{\rm R}^{\rm C}(k)$ including soft-valued $\hat{b}(l)$.

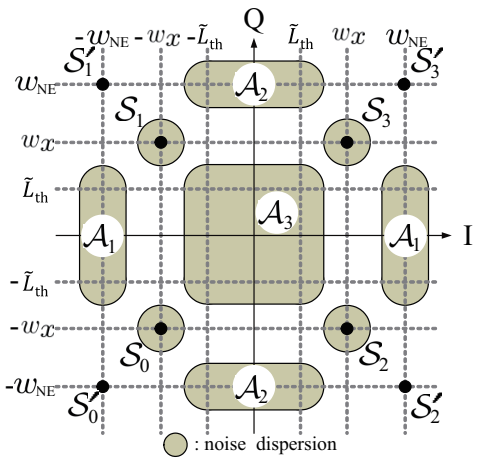

Fig. 2. An exapmple ($\Re[\xi_{\rm RD}(k)] = \Im[\xi_{\rm RD}(k)]$) of the constellations of the received symbols $y^{\rm C}_{\rm D}(k)$. $\tilde{L}_{\rm th} = L_{\rm th} w_{\rm NE}/\mu$.

An exapmple of the constellations of the received symbols $y^{\rm C}_{\rm D}(k)$ in the D node is drawn in Fig 2. PDF of $y^{\rm C}_{\rm D}(k)$ is characterized by a Gaussian mixture model. $\mathcal{S}'_q$ denotes a virtual constellation set which removes noise components from (26), resulting in $\{\mathcal{S}'_0, \mathcal{S}'_1, \mathcal{S}'_2, \mathcal{S}'_3\} = \{(-1-{\rm j})w_{\rm NE}, (-1+{\rm j})w_{\rm NE}, (1-{\rm j})w_{\rm NE}, (1+{\rm j})w_{\rm NE}\}$. In principle, according to sets of fowarded data symbols $\mathcal{S}_q$ and $\mathcal{S}'_q$, the PDFs are given by different complex-valued Gaussian distiobutions. When $\mathcal{S}_q$ is forwarded from the R node, following the DF manner, the extrinsic LLRs $\alpha^{\rm C}_{\rm D}(l)$ is readily calculated by (13). When $\mathcal{S}'_q$ is done, on the other hand, due to the noise elimination by threshold value $L_{\rm th}$, there is a possibility to include imbalanced variances between In- and Quadrature- phases as shown in Fig. 2 as areas $\mathcal{A}_1$, $\mathcal{A}_2$, and $\mathcal{A}_3$. Each PDF of received symbols $y^{\rm C}_{\rm D}(k)$ belonging to the areas is given by

$$p(y^{\rm C}_{\rm D}(k)|\mathcal{S}'_q) = \tag{27}$$
$$\begin{cases} \frac{1}{\pi\sqrt{N_0 N_{\rm NE}(k)}} \exp\left(-\frac{d^2_{\rm I}(k,\mathcal{S}'_q)}{N_0}\right) \exp\left(-\frac{d^2_{\rm Q}(k,\mathcal{S}'_q)}{N_{\rm NE}(k)}\right) : \mathcal{A}_1 \\ \frac{1}{\pi\sqrt{N_0 N_{\rm NE}(k)}} \exp\left(-\frac{d^2_{\rm I}(k,\mathcal{S}'_q)}{N_{\rm NE}(k)}\right) \exp\left(-\frac{d^2_{\rm Q}(k,\mathcal{S}'_q)}{N_0}\right) : \mathcal{A}_2 \\ \frac{1}{\pi N_{\rm NE}(k)} \exp\left(-\frac{d^2_{\rm I}(k,\mathcal{S}'_q)}{N_{\rm NE}(k)}\right) \exp\left(-\frac{d^2_{\rm Q}(k,\mathcal{S}'_q)}{N_{\rm NE}(k)}\right) : \mathcal{A}_3 \end{cases},$$

where we have

$$d_{\rm I}(k,\mathcal{S}'_q) = \Re[y^{\rm C}_{\rm D}(k)] - \Re[\xi_{\rm RD}(k)\mathcal{S}'_q], \tag{28}$$
$$d_{\rm Q}(k,\mathcal{S}'_q) = \Im[y^{\rm C}_{\rm D}(k)] - \Im[\xi_{\rm RD}(k)\mathcal{S}'_q], \tag{29}$$
$$N_{\rm NE}(k) = N_0 + 2\sigma^2_\beta |\xi_{\rm RD}(k)|^2 w^2_{\rm NE}. \tag{30}$$

This multi-modality implies a fact that the PDF for each received symbol should be identified in advance of the calculation of the extrinsic LLR $\alpha^{\rm C}_{\rm D}(l)$. The identification problem may be solved by classifications of received symbols $y^{\rm C}_{\rm D}(k)$ into areas $\mathcal{A}_0$, $\mathcal{A}_1$, $\mathcal{A}_2$ and $\mathcal{A}_3$. Note that $\mathcal{A}_0$ indicates areas for $\mathcal{S}_q$. In order to clasify the received symbols, we focus on the minimum Euclidean distance $|y^{\rm C}_{\rm D}(k) - \xi_{\rm RD}(k)\mathcal{Z}_a|^2$[1]. Table I specifies reference points $\mathcal{Z}_a$. According to PDF of the area having the minimum Euclidian ditance, as with the derivation of (6), extrinsic LLRs $\alpha^{\rm C}_{\rm D}(l)$ are given by

$$\boldsymbol{\alpha}^{\rm C}_{\rm D}(k) = \boldsymbol{\Omega}_{\rm NE}(k)\boldsymbol{\eta}_{\rm RD}(k), \tag{31}$$

where we have

$$\boldsymbol{\Omega}_{\rm NE}(k) = \begin{cases} {\rm diag}\,[w_0(k), w_{\rm NE}(k)] & : \mathcal{A}_1 \\ {\rm diag}\,[w_{\rm NE}(k), w_0(k)] & : \mathcal{A}_2 \\ {\rm diag}\,[w_{\rm NE}(k), w_{\rm NE}(k)] & : \mathcal{A}_3 \end{cases}, \tag{32}$$

with the elements defined by

$$\omega_{\rm NE}(k) = \frac{4w_x w_{\rm NE}}{N_{\rm NE}}(k), \qquad \omega_0(k) = \frac{4w_x w_{\rm NE}}{N_0}. \tag{33}$$

The operator ${\rm diag}[a,b]$ denotes a diagonal matrix. $\begin{bmatrix} a & 0 \\ 0 & b \end{bmatrix}$ For the ease of analysis, we assume a perfect notification of $w_{\rm NE}$ and σ^2_β from the R node to the D node.

TABLE I
REFERENCE POINTS $\mathcal{Z}_a$ FOR THE AREA CLASSIFICATION.

$\mathcal{A}_0$	$\Leftarrow \{\pm w_x$	$\pm {\rm j} w_x\}$
$\mathcal{A}_1$	$\Leftarrow \{\pm w_x$	$\pm {\rm j} L_{\rm th} w_{\rm NE}/\mu\}$
$\mathcal{A}_2$	$\Leftarrow \{\pm L_{\rm th} w_{\rm NE}/\mu$	$\pm {\rm j} w_x\}$
$\mathcal{A}_3$	$\Leftarrow \{\pm L_{\rm th} w_{\rm NE}/\mu$	$\pm {\rm j} L_{\rm th} w_{\rm NE}/\mu\}$

TABLE II
SIMULATION CONDITIONS.

Modulation	Gray coded QPSK
Channel Encoder	Non-Systematic Convolutional (Coding rate $R_{\rm c}$ = 1/2) (Constraint length = 4)
Channel Decoder	Max-Log-MAP with Jacobian logarithm
Frame Length K	512 symbols/frame
Interleaver	Random
LLR threshol	$L_{th} = 3.5$

IV. NUMERICAL RESULTS

In order to characterize the proposed partial noise elimination scheme for DAF relaying (NE-DAF), computer simulations have been conducted. Table II specifies major simulation conditions to be used.

Assuming that the channel is AWGN, i.e. $\xi_{\rm SR}(k) = \xi_{\rm SD}(k) = \xi_{\rm RD}(k) = 1 \ \forall \ k$, frame error rate (FER) performances as a function of $E_{\rm s}/N_0$ of the S-R link is demonstrated in Figs. 3(a) and 3(b). In order to investigate impacts of link quality of the S-R link, $E_{\rm s}/N_0$ values of S-D and R-D links were fixed to 1.0 [dB] and 6.0 [dB], respectively. The LLR threshold $L_{th} = 3.5$ was chosen as the proposed method plays the best performance in given conditions. In Fig. 3(a), MAP decoding is carried out in the R node. On the other hand, it is not done in Fig. 3(b).

Here, we focus on the comparison between DF, DAF, and NE-DAF with the aid of MAP decoding. The crossover point of FER curves of DF and DAF is around 6 [dB]. This point implies that DF manner is an excellent strategy if the link quality of S-R is relatively higher to achieve fewer bit error ($c(l) \neq \hat{c}(l)$). Otherwise, the FER performance is exacerbated by the approximation mentioned in Sect. II.C.1). In contrast to the DF performance, the DAF manner has an advantage in lower $E_{\rm s}/N_0$ of the S-R link since it is free from hard-decision error in the R node. However, as a bad news, the FER

[1]The criterion of minimum Euclidean distance is not the best way in terms of probability theory. However, for ease of analysis, we use the criterion.

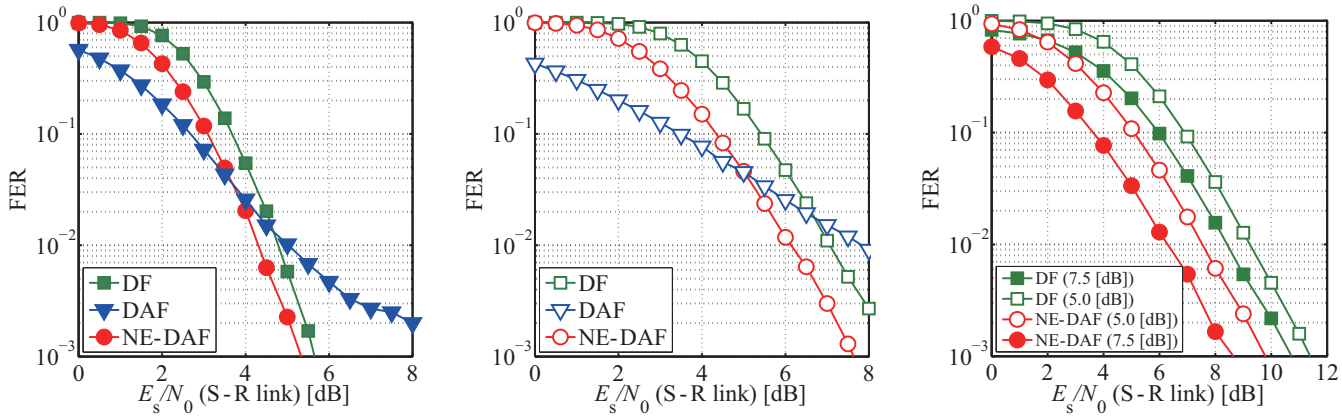

(a) With MAP decoding in the R node (AWGN). (b) Without MAP decoding in the R node (AWGN). (c) With MAP decoding in the R node (S-D, S-R: 24-path Rayleigh fading, R-D: AWGN).

Fig. 3. FER performances as a function of E_s/N_0 of the S-R link in the D node.

performance is worse than that of DF in high E_s/N_0 region. This is because noise terms are always propagated to the D node, even when high E_s/N_0 of the S-R link is guaranteed.

This crossover point brings us to a concept that DF and DAF manner should be switched for each frame according to the link quality. This frame-wise switching strategy is investigated in [6]. However, the proposed strategy by bit-wise partial noise elimination (NE-DAF) is to switch DF and DAF for each bit according to the reliability of LLRs. As a consequence of the bit-wise switching, NE-DAF outperforms DF at any E_s/N_0 of the S-R link without any crossover point. More specifically, comparing to the DF in the given simulation conditions, approximately 0.5 [dB] gain can be obtained by the NE-DAF.

Next, let us focus on the comparison between Figs. 3(a) and 3(b). We are able to find a fact that the MAP decoding in the R node is a powerful operation to improve FER performances although it requires computational burden. In this case, comparing to the DF, approximately 1.0 [dB] gain is achieved by the NE-DAF.

Eventually, in Fig. 3(c), FER performances of DF and NE-DAF manners in frequency selective fading channels are demonstrated. The channel of R-D link was assumed to be AWGN ($|\xi_{\mathrm{RD}}(k)|$=1) since we can reasonably set up the R node at the point having low frequency selectivity of the cannel. E_s/N_0 value of R-D link was fixed 6.0 [dB], and that of S-D link is described in the figure legend. In S-R and S-D links, $\xi_{\mathrm{SR}}(k)$ and $\xi_{\mathrm{SD}}(k)$ were generated by 24-path Rayleigh fading with equal power delay profile without considering path loss and shadowing. The channel estimations in the receivers are assumed to be perfect. Comparing between DF and NE-DAF, we can see 1.7 [dB] and 2.1 [dB] gains at FER=0.01 when E_s/N_0 value of S-D is 5.0 [dB] and 7.5 [dB], respectively. In comparison with AWGN scenario, higher gains are attained by a wide dynamic range of LLR distributions caused by frequency selectivity. There might be a high possibility to co-exist highly and negligibly reliable LLR in one frame, due to the dynamic range. In this case, we should proactively cut the unnecessaly noise components included in highly reliable LLRs. Thus, the importance of bit-wise partial noise elimination in OFDM scenario clearly appears.

V. Conclusion

In this paper, the bit-wise partial noise elimination scheme was proposed for DAF relaying. The main problem to be solved was to formulate a classification problem to calculate extrinsic LLRs provided by demapper in the D node. In order to address the problem, we focused on Euclid distances between received symbols and reference symbols which were investigated through this paper.

We demonstrated that the bit-wise partial noise elimination scheme is effective in terms of improving FER performances in comparison with the DF relaying.

Acknowledgment

This research was supported in part by "Global COE (Centers of Excellence) Program" of the Ministry of Education, Culture, Sports, Science and Technology, Japan, and KAKENHI (23760335), Japan.

References

[1] A. Sendonaris, E. Erkip, and B. Aazhang, "User cooperation diversity-part I: System description," *IEEE Trans. Commun.*, vol. 51, no. 11, pp. 1927–1938, Nov. 2003.

[2] A. Nosratinia, T. E. Hunter, and A. Hedayat, "Cooperative communication in wireless networks," *IEEE Commun. Mag.*, vol. 42, no. 10, pp. 68–73, Oct. 2004.

[3] J. Laneman, D. Tse, and G. Wornell, "Cooperative diversity in wireless networks: Efficient protocols and outage behavior," *IEEE Trans. Inform. Theory*, vol. 50, no. 11, pp. 3062–3080, Dec. 2004.

[4] E. Meulen, "Three-terminal communication channels," *Adv. Appl. Probability*, vol. 3, no. 1, pp. 120–154, Spring 1971.

[5] T. Cover and A. E. Gamal, "Capacity theorems for the relay channel," *IEEE Trans. Inform. Theory*, vol. IT-25, pp. 572–584, Sept. 1979.

[6] J. Fricke, M. Butt, and P. Hoeher, "Quality oriented adaptive forwarding for wireless relaying," *IEEE Commun. Lett.*, vol. 12, no. 3, pp. 200–202, Mar. 2008.

[7] X. Bao and J. Li, "Efficient message relaying for wireless user cooperation: Decode-amplify-forward (DAF) and hybrid DAF and coded-cooperation," *IEEE Trans. Wireless Commun.*, vol. 6, no. 11, pp. 3975–3984, Nov. 2007.

[8] S. ten Brink, "Convergence behavior of iteratively decoded parallel concatenated codes,," *IEEE Trans. Commun.*, vol. 49, no. 10, pp. 1727–1737, Oct. 2001.

[9] J. Hagenauer, "The turbo principle in mobile communications," in *Proc. ISITA*, XI'AN, Peoples Republic of China, Oct. 2002.